Early Diagnosis and Detection of Progression

Yong Woo Kim

Abstract

Glaucoma is one of the leading causes of blindness. It is a progressive disease with differing rates of progression among individuals. Since the severity of the disease at presentation is a major risk factor for glaucoma blindness, early diagnosis and detection of progression is critical to prevention of blindness due to glaucoma. This chapter provides an overview on the utility of optical coherence tomography (OCT) imaging for early detection of glaucomatous structural damage and progression, with relevant clinical cases. The OCT devices enable not only thickness measurement of each retinal layer but also topographical analysis of glaucomatous damage based on deviation and/or thickness maps. Clinicians can use built-in Guided Progression Analysis (GPA) software to detect structural change and estimate the rate of progression. This chapter offers the latest knowledge along with practical tips for interpreting OCT printouts for early diagnosis and monitoring of glaucomatous damage.

Keywords

Optical coherence tomography · Early diagnosis · Progression analysis · RNFL thickness · Neuroretinal rim thickness Macular GCIPL thickness

1 Early Diagnosis of Glaucoma

1.1 OCT Thickness Analysis

Optical coherence tomography (OCT) devices can provide objective and reproducible thicknesses of each retinal layer including the retinal nerve fiber layer (RNFL), ganglion cell layer (GCL), and inner plexiform layer (IPL). The measurement data are compared with the internally built-in normative database and color coded accordingly as green (normal range), yellow (< 5 percentile), red (< 1 percentile), or white (thicker than normal range). These thickness profiles can be utilized to detect early-glaucomatous structural damage.

1.1.1 RNFL Thickness

OCT-measured peripapillary RNFL thickness has been shown to be effective in discriminating preperimetric glaucoma from glaucoma-suspect eyes (Lisboa et al. 2012). Figure 1 provides a representative case of early diagnosis of glaucoma from peripapillary RNFL thickness. The infero-

Y. W. Kim (✉)
Department of Ophthalmology, Seoul National University Hospital, Jongno-gu, Seoul, Korea
e-mail: yongwookim@snu.ac.kr

K. H. Park, T.-W. Kim (eds.), *OCT Imaging in Glaucoma*,
https://doi.org/10.1007/978-981-16-1178-0_4

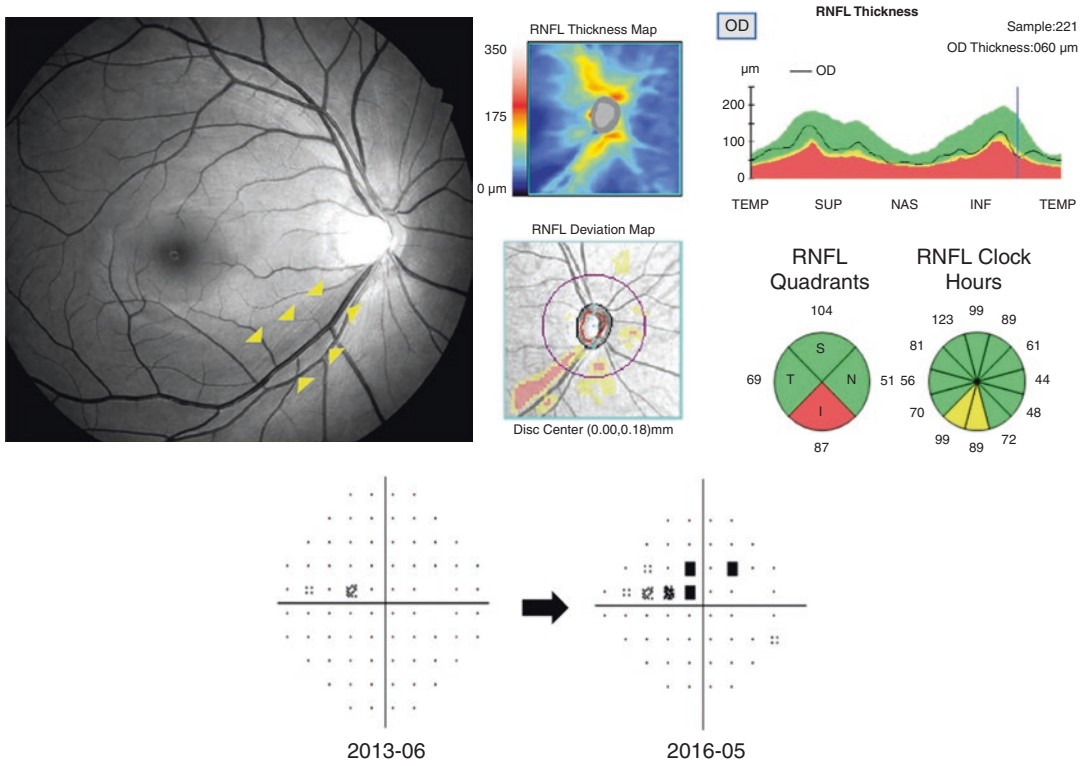

Fig. 1 Peripapillary RNFL thinning in preperimetric glaucoma. Optic disc cube scan of 40-year-old male with preperimetric glaucoma. The inferotemporal retinal nerve fiber layer (RNFL) defect in the red-free RNFL photography is well reflected in the optical coherence tomography (OCT) thickness profiles. The sectoral analysis of RNFL thickness revealed the red-color code (less than 1 percentile relative to normative database) in the inferior quadrant. The 12-hour sectoral analysis revealed the yellow-color code (less than 5 percentile of normative database) in the 6 and 7 o'clock sectors. Subsequent visual field loss appeared after 3 years, showing a superior arcuate defect

temporal RNFL defect in the red-free RNFL photography is well reflected in the OCT thickness profiles. The sectoral analysis of RNFL thickness returned the red-color code for the inferior quadrant. The 12 clock-hour sectoral analysis returned the yellow-color code for the 6 and 7 o'clock sectors. The patient, who had a within normal range visual field, showed progressive visual field defect in the corresponding superior hemifield. As shown in Fig. 1, peripapillary RNFL thickness effectively detects early structural glaucomatous damage prior to the presence of visual field defect. However, several studies have reported unsatisfactory sensitivity of peripapillary RNFL thickness, when averaged in quadrants or clock-hour sectors, for detection of localized RNFL defects in preperimetric glaucoma (Jeoung and Park 2010; Rao et al. 2013; Jeoung et al. 2014). One reported sensitivity for localized RNFL defect was 59.5% (Jeoung et al. 2014). Earlier studies reported that RNFL defects with narrow angular width are less likely to be detected on sector maps (Jeoung and Park 2010; Nukada et al. 2011). This phenomenon often occurs when clinicians solely look at the color coded sector map but not the TSNIT thickness profile graph from the OCT printout. Jeoung et al. (2014) demonstrated substantial improvement of sensitivity (up to 83.8%) for localized RNFL defect when using the TSNIT thickness graph. Figure 2 provides a representative case of preperimetric glaucoma with inferotemporal RNFL defect. In this case, the quadrant map showed "within normal range" and the 12 clock-

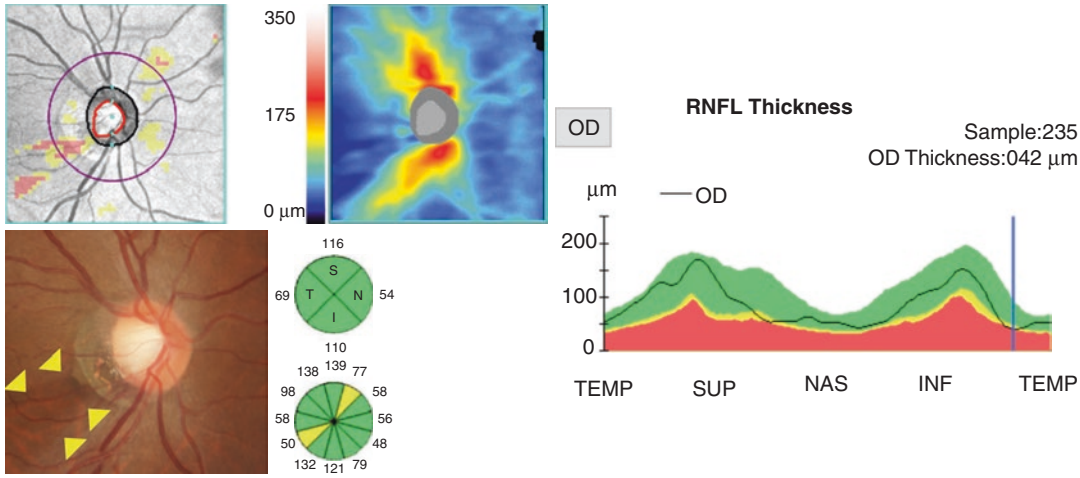

Fig. 2 TSNIT graph for early detection of glaucoma. Optic disc cube scan of 45-year-old female with preperimetric glaucoma on right eye. Note the optic disc rim narrowing and retinal nerve fiber layer (RNFL) defect (yellow triangle) in the inferotemporal region. The quadrant map showed within the normal range, and the 12-hour sector map showed only yellow color in the 8 o'clock sector. However, the TSNIT thickness graph clearly demonstrated a focal defect (thickness 42 µm) in the inferotemporal region (light blue solid line)

hour sector map showed "only yellow color" at the 8 o'clock sector. However, the TSNIT thickness graph clearly demonstrated the focal defect in the inferotemporal region.

1.1.2 Macular Parameters

The latest OCT devices provide measurement of macular ganglion cell complex (GCC, sum of macular RNFL, GCL, and IPL thickness) or ganglion cell-inner plexiform layer (GCIPL) thickness (sum of macular GCL and IPL). The macular parameters are also known to be effective in discriminating early-glaucomatous structural damage from healthy eyes. Several studies have reported that macular GCIPL or GCC showed comparable diagnostic ability for early glaucoma (Mwanza et al. 2012; Akashi et al. 2013; Jeoung et al. 2013). Mwanza et al. (2012) reported that minimum GCIPL thickness was the best parameter for discriminating early-glaucomatous change from normal eyes. Inferotemporal macular GCIPL thickness is known to be the best parameter for discriminating myopic preperimetric glaucoma from healthy myopic eyes (Seol et al. 2015). A representative case of preperimetric glaucoma with macular damage in the inferotemporal region is provided in Fig. 3. This case featured the inaugural use of the 12 × 9 mm^2-sized wide-field map from swept-source OCT (SS-OCT), which enables combined macular parameter/peripapillary RNFL thickness analysis.

However, some researchers have reported that macular GCIPL thickness showed only moderate diagnostic ability for discriminating preperimetric glaucoma from healthy eyes, and in fact, that it had even less diagnostic power than that of peripapillary RNFL or optic nerve head (ONH) parameters (Rao et al. 2013; Lisboa et al. 2013; Begum et al. 2014). This phenomenon possibly arose from the fact that macular scanning is limited to a 6 × 6 mm^2 area centered around the fovea, and as such, cannot detect any localized RNFL defect beyond this scanning area. It has been demonstrated that the diagnostic utility of GCIPL improves significantly if the RNFL defect is closer to the fovea (Kim et al. 2014; Hwang et al. 2014). A recent study compared the diagnostic ability of macular parameters between spectral-domain OCT (Cirrus HD-OCT, Carl Zeiss Meditec, Inc., Dublin, CA, USA) and swept-source OCT (SS-OCT, Triton DRI OCT, Topcon, Tokyo, Japan) for glaucomatous structural damage in myopic eyes. It confirmed that

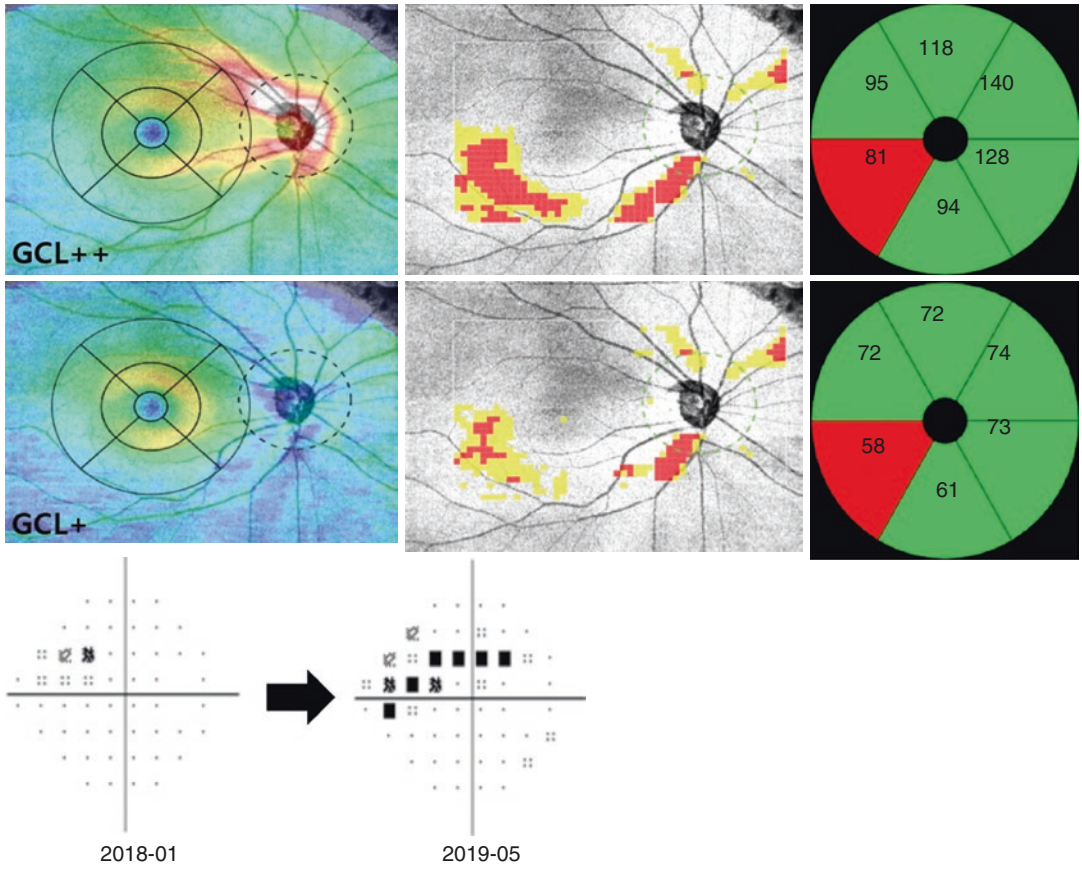

Fig. 3 Macular damage in preperimetric glaucoma. Wide-field analysis for macular and peripapillary region of 54-year-old female with preperimetric glaucoma. The 12 × 9 mm²-sized wide-field maps for GCL++ (upper row) and GCL+ (bottom row) from swept-source optical coherence tomography (SS-OCT) are provided. The wide-field map can also provide a combined SuperPixel map of peripapillary retinal nerve fiber layer (RNFL) and macular GCL++/GCL+ map (second column). Note the significant thinning in the inferotemporal sectors of both GCL++ and GCL+ at the baseline, and the progressive superior visual field defect 1 year later. GCL++: sum of macular retinal nerve fiber layer (RNFL), ganglion cell layer (GCL), and inner plexiform layer (IPL); GCL+: sum of macular GCL and IPL

SS-OCT, with a larger macular scan area than that of SD-OCT, had better glaucoma-diagnostic performance (Kim et al. 2020a).

1.1.3 Neuroretinal Rim Parameters

The neuroretinal rim parameters such as Bruch's membrane opening minimum rim width (BMO-MRW) in Spectralis OCT (Heidelberg Engineering, Heidelberg, Germany) or three-dimensional neuroretinal rim thickness (3D-NRT) in Cirrus HD-OCT (Carl Zeiss Meditec, Dublin, CA, USA) are other essential OCT parameters for glaucoma diagnosis. The BMO-MRW is defined as the minimum distance between the Bruch's membrane opening (BMO) and the internal limiting membrane. Cirrus HD-OCT detects the minimum area of a surface from the optic disc margin (defined as the BMO) to the vitreoretinal interface (VRI) based on 3D volume scan data. The 3D-NRT is defined as the distance between the BMO and VRI, which is associated with the minimum cross-sectional rim area in the given direction. These parameters are known to have comparable diagnostic ability for glaucoma (Chauhan et al. 2013; Kim and Park 2018). Figure 4 shows a representative case of early glaucoma with BMO-MRW thinning.

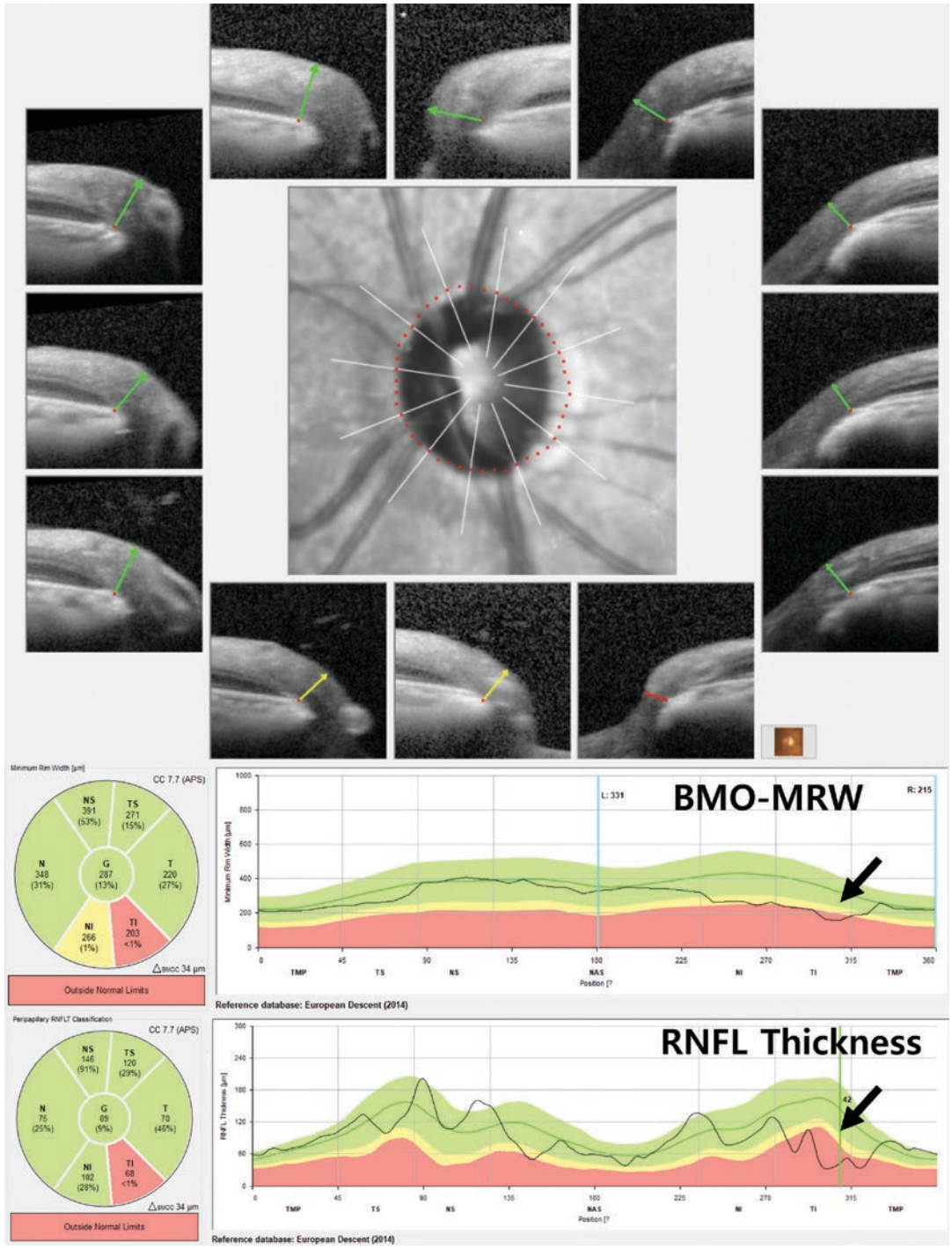

Fig. 4 BMO-MRW thinning in early glaucoma. Left eye of 43-year-old female with early open-angle glaucoma (mean deviation of visual field, –0.41 dB). Note the Bruch's membrane opening minimum rim width (BMO-MRW) as well as the decreased retinal nerve fiber layer (RNFL) thickness in the inferotemporal region

There is no doubt that the peripapillary RNFL thickness and macular parameters are essential for OCT diagnosis and monitoring of glaucoma. However, false-positive signs for these parameters are encountered in real clinical practice. False-positive rates have been reported to be as high as 30.8% for peripapillary RNFL thickness and 40.4% for macular GCIPL thickness (Kim et al. 2011, 2015a). In these studies, greater axial length and small disc area were associated with false-positive red signs for peripapillary RNFL thickness, and greater axial length and fovea-disc angle were determined to be risk factors for false positivity in macular GCIPL thickness (Kim et al. 2011, 2015a). The neuroretinal rim parameters, alternatively, can be referenced as to reduce false positives in glaucoma diagnosis, particularly in myopic eyes (Kim and Park 2018; Malik et al. 2016). Figure 5 shows the examples of false-positive red signs of peripapillary RNFL thickness in a myopic eye. The BMO-MRW from Spectralis OCT, however, revealed an intact neuroretinal rim within the normal range. This parameter is less affected by temporal migration of major vessels or scan-circle misalignment in myopic eyes. In this light, the neuroretinal rim parameters can be used complementarily to peripapillary RNFL or macular GCIPL thicknesses in detecting early-glaucomatous damage with improved specificity.

1.2 OCT Topographical Analysis

Recent advances in OCT scanning speed have enabled topographical analysis of glaucomatous damage from thickness or deviation maps of peripapillary RNFL and macular GCIPL. The peripapillary RNFL deviation map significantly improved the diagnostic sensitivity for glaucoma and provided additional spatial information for RNFL damage (Leung et al. 2010). Another study reported that the RNFL thickness map demonstrated the best diagnostic ability in detecting localized RNFL defects (Hwang et al. 2013). The temporal raphe sign from the macular GCIPL thickness map, a straight line on the horizontal raphe longer than one-half of the length between

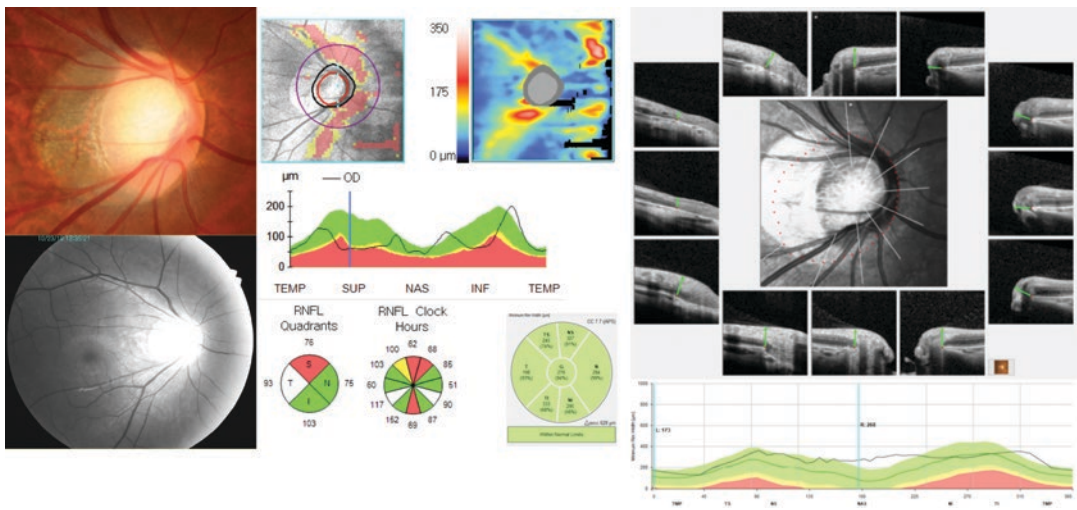

Fig. 5 False positives of RNFL thickness in myopic eyes. Cirrus HD-OCT (Carl Zeiss Meditec, Inc., Dublin, CA, USA) and Spectralis OCT (Heidelberg Engineering, Heidelberg, Germany) scan of 27-year-old healthy male with high myopia in right eye. His refraction was –11 diopters and the axial length was 30.47 mm. Optic disc and red-free retinal nerve fiber layer (RNFL) photography showed no abnormalities (left column). The RNFL deviation map as well as the quadrant and clock-hour maps showed red signs (central column). However, the Bruch's membrane opening minimum rim width (BMO-MRW) from Spectralis OCT was revealed to be within the normal range. The red-sign indications of RNFL thickness may have originated from migration of RNFL peaks and major vessels in the temporal direction

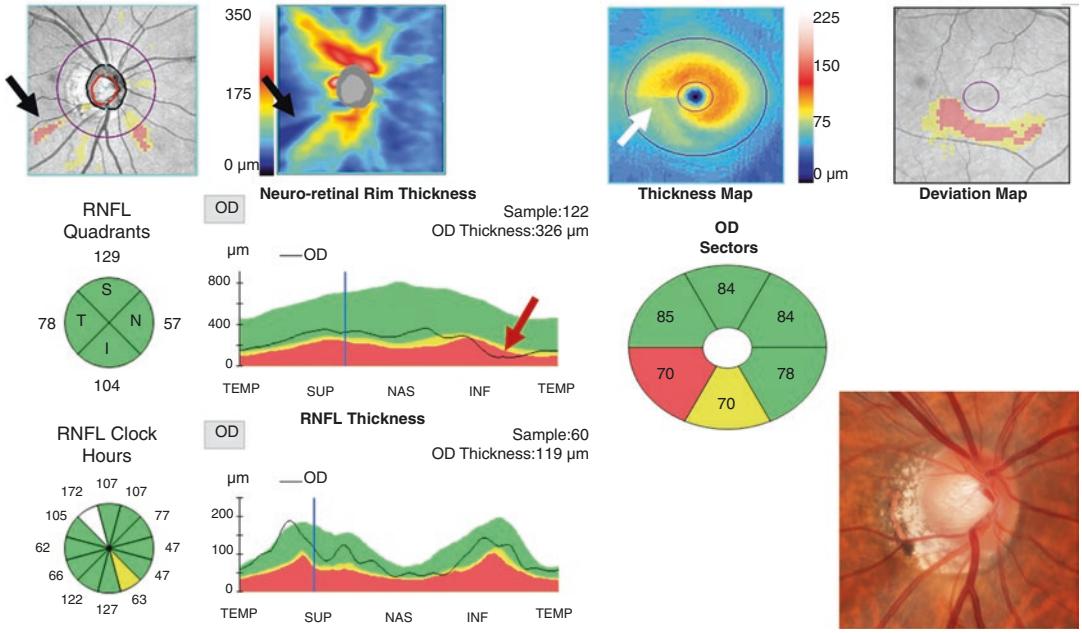

Fig. 6 Utility of OCT thickness map in detecting early-glaucomatous damage. Optic disc and macular cube scans of 40-year-old male with preperimetric glaucoma in right eye. The retinal nerve fiber layer (RNFL) quadrant and clock-hour thickness maps showed no red signs. However, the RNFL thickness and deviation maps showed RNFL defect in the inferotemporal region (black arrows). This finding is further confirmed by the three-dimensional neuroretinal rim thickness (3D-NRT, dark red arrow) and the macular ganglion cell-inner plexiform layer (GCIPL) thinning in the inferotemporal region. Note the straight line on the horizontal raphe longer than one-half of the length between the inner and outer annulus in the temporal elliptical area on the GCIPL thickness map (temporal raphe sign, white arrow)

the inner and outer annulus in the temporal elliptical area, can discriminate glaucomatous damage even in challenging cases such as highly myopic eyes (Kim et al. 2015b, 2016). Figure 6 shows a representative case that highlights the usefulness of the peripapillary RNFL thickness map in detecting early-glaucomatous change. In this case, the quadrant and clock-hour RNFL maps as well as the TSNIT thickness graph showed normal ranges of measurements, but the RNFL thickness map exhibited the localized defect in the inferotemporal region. The 3D-NRT and GCIPL thickness maps further confirmed the structural damage in this case.

The latest commercially available SS-OCT (DRI OCT Triton, Topcon, Tokyo, Japan) can capture a wider area of the retina (12×9 mm^2) in a single scan, thus providing a "wide-field map." The wide-field thickness and SuperPixel map has been shown to be effective in discriminating preperimetric and early-perimetric glaucoma from healthy eyes (Lee et al. 2017a). The wide-field Superpixel map was superior even to that of the RNFL deviation map from Cirrus HD-OCT (Lee et al. 2018a). The wide-field thickness surface map is displayed in 3D for selected layers (RNFL, GCL++, or GCL+) and can be rotated or zoomed in and out by mouse operation. This map enables detection of localized RNFL defects intuitively easy. Figure 7 shows the benefits of the wide-field map when detecting a localized superior-hemifield RNFL defect that most conventional SD-OCT macular scans would not find.

2 Detection of Progression

Glaucoma progression varies greatly from person to person, ranging from rapid to slow (Heijl et al. 2009, 2013). It can continue to show progression

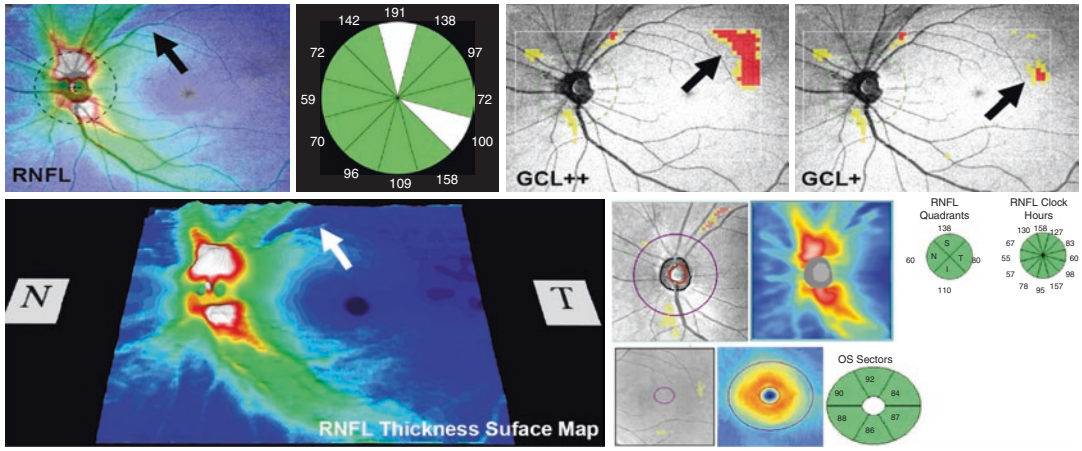

Fig. 7 Utility of wide-field map in detecting early-glaucomatous damage. Wide-field map scanned from 49-year-old male with early glaucoma in left eye (mean deviation of visual field, –3.11 dB). The wide-field map detected the localized retinal nerve fiber layer (RNFL) defect in the superotemporal region (black and white arrows). However, scans from the same eye by spectral-domain OCT (Cirrus HD-OCT, Carl Zeiss Meditec, Inc., Dublin, CA, USA) did not detect any structural damage, due possibly to the limited scan area (green box)

despite treatment, even within the normal range of intraocular pressure (Collaborative Normal-Tension Glaucoma Study Group 1998). Therefore, tonometry alone cannot be sufficient in monitoring glaucoma. OCT is a reliable tool for detection of structural progression and monitoring of the rate of change. Although glaucoma progression analysis is focused mainly on the peripapillary RNFL, recent OCT devices, such as BMO-MRW and 3D-NRT, also provide tools for monitoring of macular GCIPL or neuroretinal rim thickness.

2.1 RNFL Progression Analysis

Progressive RNFL thinning in glaucoma can be assessed on OCT scans either by comparing RNFL thickness between the baseline and selected follow-up images (event-based analysis) or by estimating the rate of RNFL thinning in a linear regression model from a series of OCT scans (trend-based analysis). While these kinds of analysis can be done manually by individual clinicians, they can be prohibitively time-consuming in a busy clinical setting. The latest OCT devices provide automated proprietary software tools for progression analysis, but different OCT brands have slightly different features. Guided Progression Analysis (GPA™) from Cirrus HD-OCT is unique in that it provides topographical event-based RNFL thickness change over the 6 × 6 mm^2 peripapillary region (Fig. 8). It allows the user to analyze between 3 and 8 exams and determines if statistically significant change has occurred. The earliest two exams are set as the baselines, and later exams are compared with them for determination of any significant change. Follow-up scans are aligned to the baselines based on the blood vessels or center of optic disc identified in the *en face* images (Cirrus HD-OCT User Manual). In event-based analysis, "Possible Loss" is declared and encoded in yellow when the individual plot has changed, relative to the two baseline exams, by a greater extent than the test-retest variability for a single visit. "Likely Loss" is declared and encoded in red when significant change has been detected on two visits in a row. "Possible Increase" is declared and encoded in lavender when the rate of gain is significant. In trend-based analysis, the slope is estimated by linear regression and is displayed in "μm/year" with the 95% confidence interval. This will be provided whenever at least 4 exams spanning at least 2 years are loaded. The linear regression line is plotted on each graph whenever

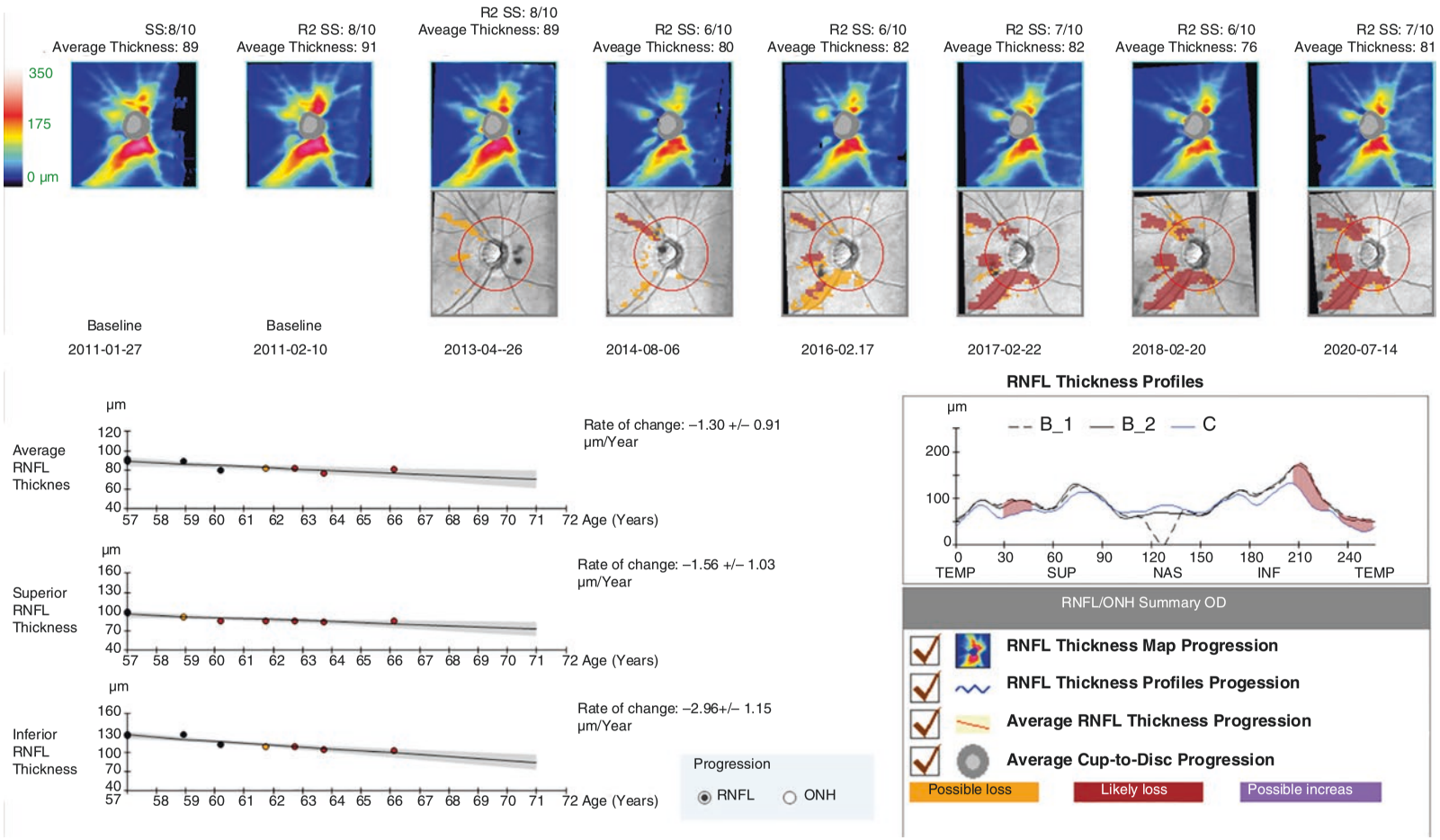

Fig. 8 RNFL progression analysis. Guided Progression Analysis (GPA™) from Cirrus HD-OCT detects event-based RNFL thickness change over the 6 × 6 mm² peripapillary region and estimates trend-based rates of change for average, superior, and inferior peripapillary RNFL thicknesses. The serial optic disc scans from a 57-year-old female with open-angle glaucoma and a history of recurrent disc hemorrhage showed significant progression ("Likely Loss") at the superotemporal, inferotemporal, and temporal regions. The rate of average retinal nerve fiber layer (RNFL) thinning was –1.30 ± 0.91 µm/year

there is both "Likely Loss" and a significant linear trend ($P < 5\%$). Other OCT brands can also automatically estimate and report the slope of RNFL thinning with statistical significance. Statistically significant *P*-values do not always mean that there is clinically significant "progression." Even small, clinically insignificant changes can be statistically significant in a series of large-scale OCT scans; and, vice versa, if the number of OCT images is small and of poor quality, a clinically significant change can be determined as insignificant ($P > 0.05$).

Monitoring of peripapillary RNFL thickness with OCT has been shown to be effective in detecting glaucomatous damage prior to the appearance of visual field defect (Kuang et al. 2015). Furthermore, OCT has been reported to be more sensitive than standard automated perimetry in detecting progression in the early stages of glaucoma (Wollstein et al. 2005; Zhang et al. 2017). It is therefore imperative to monitor progressive RNFL thinning by OCT, the findings of which are informative for prediction of future visual field loss in glaucoma (Yu et al. 2016; Lin et al. 2017).

2.2 GCIPL Progression Analysis

Progression analysis for macular GCIPL is also available in both event- and trend-based modes. Glaucoma patients who had shown progression on serial red-free RNFL photographs or automated perimetry had a significantly faster thinning rate of macular GCIPL than that of non-progressors (Lee et al. 2017b, c). In a dynamic range-normalized analysis, the rate of peripapillary RNFL thinning was faster than that of macular GCIPL (Hammel et al. 2017). Nevertheless, progressive macular GCIPL thinning and progressive peripapillary RNFL thinning were found to be mutually predictive, and were both indicative of visual field progression (Hou et al. 2018; Shin et al. 2020). In this sense, integrating progressive peripapillary RNFL and macular GCIPL thinning may be advantageous to progression analysis in glaucoma (Lee et al. 2018b, c; Wu et al. 2020).

Monitoring the macular GCIPL thickness in a topographical manner has improved our understanding of macular damage patterns in glaucoma. Macular GCIPL defect in one study was most commonly found in the inferotemporal region relative to the fovea (Shin et al. 2018). In that investigation, GPA™ analysis showed that the region toward the fovea and optic disc from the initial inferotemporal GCIPL defect was the most frequent site for progression. The most common pattern of progressive thinning, meanwhile, was widening of GCIPL defect, followed by deepening and newly developed GCIPL (Shin et al. 2018).

Monitoring macular GCIPL is advantageous to detection of progression in advanced glaucoma eyes when peripapillary RNFL thickness reaches the measurement floor (Hammel et al. 2017; Shin et al. 2017; Lavinsky et al. 2018). Figure 9 demonstrates the utility of monitoring progressive macular GCIPL thinning in advanced glaucoma eyes. The macular damage that causes GCIPL thinning might occur in the later stages of disease and at a different rate relative to peripapillary RNFL thinning. But given that a floor effect on macular GCIPL may also exist, the utility of macular GCIPL monitoring in advanced glaucoma may be limited for some patients.

2.3 BMO-MRW Progression Analysis

Spectralis OCT provides progression analysis reporting for BMO-MRW. Figure 10 shows a representative case with progressive BMO-MRW thinning in an open-angle glaucoma eye with recurrent disc hemorrhage. In a longitudinal analysis of glaucoma eyes with disc hemorrhage, the BMO-MRW showed progressive thinning, and the inferotemporal sector showed the highest rate of change (Cho and Kee 2020). Cirrus HD-OCT's 3D-NRT also showed a faster rate of thinning at the site of hemorrhage than in the other sectors (Kim et al. 2020b). The clinical utility of analyzing progressive change of neuroretinal rim parameters requires further elucidation in terms of glaucoma monitoring.

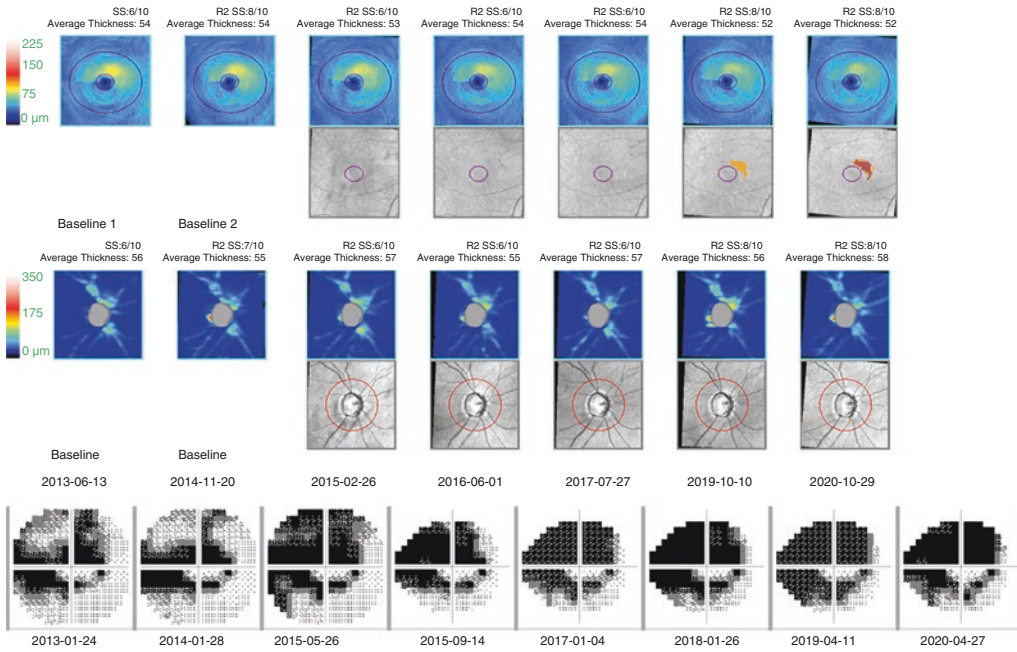

Fig. 9 GCIPL progression analysis. Guided Progression Analysis (GPA™) of macular ganglion cell-inner plexiform layer (GCIPL) and peripapillary retinal nerve fiber layer (RNFL) thicknesses from 53-year-old male with advanced glaucoma (baseline mean deviation of visual field [VF], –18.79 dB). Note the progressive thinning of the macular GCIPL ("Likely Loss" at superior parafovea) and note also the fact that the diffuse atrophied RNFL reached to the measurement floor and did not show any significant change ("floor effect"). The VF progressed significantly from –18.79 to –23.17 dB during the observation period

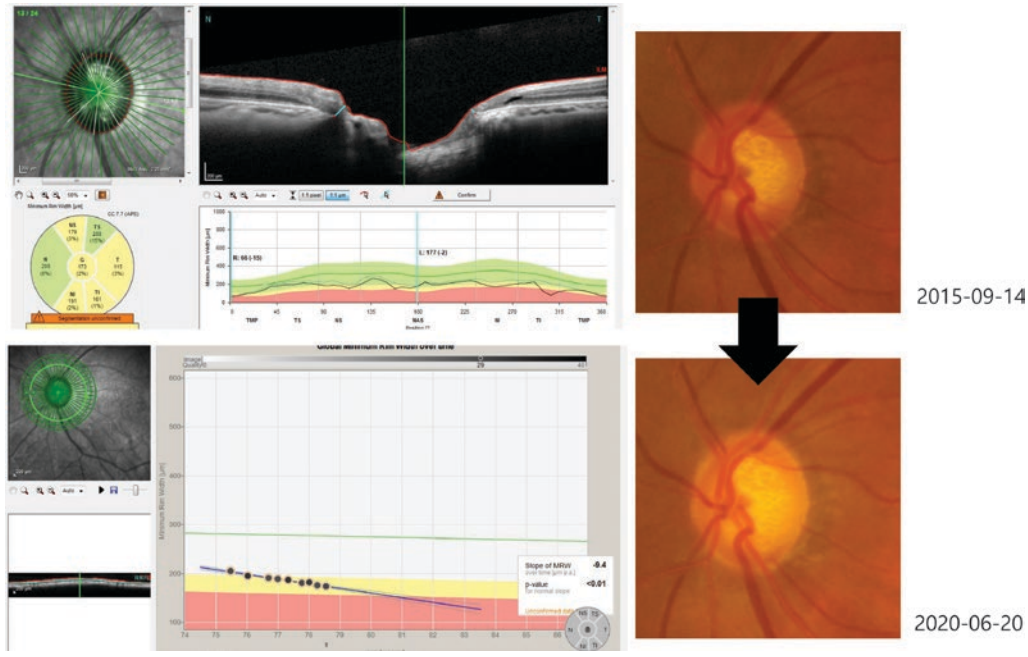

Fig. 10 BMO-MRW progression analysis. Spectralis OCT scan from 57-year-old female with open-angle glaucoma and history of recurrent disc hemorrhage in inferotemporal region of left eye. The progression analysis demonstrated significant thinning of the BMO-MRW (rate of change, –9.4 µm/year, $P < 0.01$)

References

Akashi A, Kanamori A, Nakamura M, Fujihara M, Yamada Y, Negi A. Comparative assessment for the ability of Cirrus, RTVue, and 3D-OCT to diagnose glaucoma. Invest Ophthalmol Vis Sci. 2013;54(7):4478–84.

Begum VU, Addepalli UK, Yadav RK, et al. Ganglion cell-inner plexiform layer thickness of high definition optical coherence tomography in perimetric and preperimetric glaucoma. Invest Ophthalmol Vis Sci. 2014;55(8):4768–75.

Chauhan BC, O'Leary N, AlMobarak FA, et al. Enhanced detection of open-angle glaucoma with an anatomically accurate optical coherence tomography-derived neuroretinal rim parameter. Ophthalmology. 2013;120(3):535–43.

Cho HK, Kee C. Comparison of rate of change between bruch's membrane opening minimum rim width and retinal nerve fiber layer in eyes showing optic disc hemorrhage. Am J Ophthalmol. 2020;217:27–37.

Cirrus HD-OCT User Manual 2660021159751 Rev. A 2015-08. Appendix A.

Collaborative Normal-Tension Glaucoma Study Group. Comparison of glaucomatous progression between untreated patients with normal-tension glaucoma and patients with therapeutically reduced intraocular pressures. Am J Ophthalmol. 1998;126(4):487–97.

Hammel N, Belghith A, Weinreb RN, Medeiros FA, Mendoza N, Zangwill LM. Comparing the rates of retinal nerve fiber layer and ganglion cell-inner plexiform layer loss in healthy eyes and in glaucoma eyes. Am J Ophthalmol. 2017;178:38–50.

Heijl A, Bengtsson B, Hyman L, Leske MC. Natural history of open-angle glaucoma. Ophthalmology. 2009;116(12):2271–6.

Heijl A, Buchholz P, Norrgren G, Bengtsson B. Rates of visual field progression in clinical glaucoma care. Acta Ophthalmol. 2013;91(5):406–12.

Hou HW, Lin C, Leung CK. Integrating macular ganglion cell inner plexiform layer and parapapillary retinal nerve fiber layer measurements to detect glaucoma progression. Ophthalmology. 2018;125(6):822–31.

Hwang YH, Kim YY, Kim HK, Sohn YH. Ability of cirrus high-definition spectral-domain optical coherence tomography clock-hour, deviation, and thickness maps in detecting photographic retinal nerve fiber layer abnormalities. Ophthalmology. 2013;120(7):1380–7.

Hwang YH, Jeong YC, Kim HK, Sohn YH. Macular ganglion cell analysis for early detection of glaucoma. Ophthalmology. 2014;121(8):1508–15.

Jeoung JW, Park KH. Comparison of Cirrus OCT and Stratus OCT on the ability to detect localized retinal nerve fiber layer defects in preperimetric glaucoma. Invest Ophthalmol Vis Sci. 2010;51(2):938–45.

Jeoung JW, Choi YJ, Park KH, Kim DM. Macular ganglion cell imaging study: glaucoma diagnostic accuracy of spectral-domain optical coherence tomography. Invest Ophthalmol Vis Sci. 2013;54(7):4422–9.

Jeoung JW, Kim TW, Weinreb RN, Kim SH, Park KH, Kim DM. Diagnostic ability of spectral-domain versus time-domain optical coherence tomography in preperimetric glaucoma. J Glaucoma. 2014;23(5):299–306.

Kim YW, Park KH. Diagnostic accuracy of three-dimensional neuroretinal rim thickness for differentiation of myopic glaucoma from myopia. Invest Ophthalmol Vis Sci. 2018;59(8):3655–66.

Kim NR, Lim H, Kim JH, Rho SS, Seong GJ, Kim CY. Factors associated with false positives in retinal nerve fiber layer color codes from spectral-domain optical coherence tomography. Ophthalmology. 2011;118(9):1774–81.

Kim MJ, Jeoung JW, Park KH, Choi YJ, Kim DM. Topographic profiles of retinal nerve fiber layer defects affect the diagnostic performance of macular scans in preperimetric glaucoma. Invest Ophthalmol Vis Sci. 2014;55(4):2079–87.

Kim KE, Jeoung JW, Park KH, Kim DM, Kim SH. Diagnostic classification of macular ganglion cell and retinal nerve fiber layer analysis: differentiation of false-positives from glaucoma. Ophthalmology. 2015a;122(3):502–10.

Kim YK, Yoo BW, Kim HC, Park KH. Automated detection of hemifield difference across horizontal raphe on ganglion cell-inner plexiform layer thickness map. Ophthalmology. 2015b;122(11):2252–60.

Kim YK, Yoo BW, Jeoung JW, Kim HC, Kim HJ, Park KH. Glaucoma-diagnostic ability of ganglion cell-inner plexiform layer thickness difference across temporal raphe in highly myopic eyes. Invest Ophthalmol Vis Sci. 2016;57(14):5856–63.

Kim YW, Lee J, Kim JS, Park KH. Diagnostic accuracy of wide-field map from swept-source optical coherence tomography for primary open-angle glaucoma in myopic eyes. Am J Ophthalmol. 2020a;218:182–91.

Kim YW, Lee WJ, Seol BR, Kim YK, Jeoung JW, Park KH. Rate of three-dimensional neuroretinal rim thinning in glaucomatous eyes with optic disc haemorrhage. Br J Ophthalmol. 2020b;104(5):648–54.

Kuang TM, Zhang C, Zangwill LM, Weinreb RN, Medeiros FA. Estimating lead time gained by optical coherence tomography in detecting glaucoma before development of visual field defects. Ophthalmology. 2015;122(10):2002–9.

Lavinsky F, Wu M, Schuman JS, et al. Can macula and optic nerve head parameters detect glaucoma progression in eyes with advanced circumpapillary retinal nerve fiber layer damage? Ophthalmology. 2018;125(12):1907–12.

Lee WJ, Na KI, Kim YK, Jeoung JW, Park KH. Diagnostic Ability of wide-field retinal nerve fiber layer maps using swept-source optical coherence tomography for detection of preperimetric and early perimetric glaucoma. J Glaucoma. 2017a;26(6):577–85.

Lee WJ, Kim YK, Park KH, Jeoung JW. Evaluation of ganglion cell-inner plexiform layer thinning in eyes with optic disc hemorrhage: a trend-based

progression analysis. Invest Ophthalmol Vis Sci. 2017b;58(14):6449–56.

Lee WJ, Kim YK, Park KH, Jeoung JW. Trend-based analysis of ganglion cell-inner plexiform layer thickness changes on optical coherence tomography in glaucoma progression. Ophthalmology. 2017c;124(9):1383–91.

Lee WJ, Oh S, Kim YK, Jeoung JW, Park KH. Comparison of glaucoma-diagnostic ability between wide-field swept-source OCT retinal nerve fiber layer maps and spectral-domain OCT. Eye (Lond). 2018a;32(9):1483–92.

Lee WJ, Kim TJ, Kim YK, Jeoung JW, Park KH. Serial combined wide-field optical coherence tomography maps for detection of early glaucomatous structural progression. JAMA Ophthalmol. 2018b;136(10):1121–7.

Lee WJ, Na KI, Ha A, Kim YK, Jeoung JW, Park KH. Combined use of retinal nerve fiber layer and ganglion cell-inner plexiform layer event-based progression analysis. Am J Ophthalmol. 2018c;196:65–71.

Leung CK, Lam S, Weinreb RN, et al. Retinal nerve fiber layer imaging with spectral-domain optical coherence tomography: analysis of the retinal nerve fiber layer map for glaucoma detection. Ophthalmology. 2010;117(9):1684–91.

Lin C, Mak H, Yu M, Leung CK. Trend-based progression analysis for examination of the topography of rates of retinal nerve fiber layer thinning in glaucoma. JAMA Ophthalmol. 2017;135(3):189–95.

Lisboa R, Leite MT, Zangwill LM, Tafreshi A, Weinreb RN, Medeiros FA. Diagnosing preperimetric glaucoma with spectral domain optical coherence tomography. Ophthalmology. 2012;119(11):2261–9.

Lisboa R, Paranhos A Jr, Weinreb RN, Zangwill LM, Leite MT, Medeiros FA. Comparison of different spectral domain OCT scanning protocols for diagnosing preperimetric glaucoma. Invest Ophthalmol Vis Sci. 2013;54(5):3417–25.

Malik R, Belliveau AC, Sharpe GP, Shuba LM, Chauhan BC, Nicolela MT. Diagnostic accuracy of optical coherence tomography and scanning laser tomography for identifying glaucoma in myopic eyes. Ophthalmology. 2016;123(6):1181–9.

Mwanza JC, Durbin MK, Budenz DL, et al. Glaucoma diagnostic accuracy of ganglion cell-inner plexiform layer thickness: comparison with nerve fiber layer and optic nerve head. Ophthalmology. 2012;119(6):1151–8.

Nukada M, Hangai M, Mori S, et al. Detection of localized retinal nerve fiber layer defects in glaucoma using enhanced spectral-domain optical coherence tomography. Ophthalmology. 2011;118(6):1038–48.

Rao HL, Addepalli UK, Chaudhary S, et al. Ability of different scanning protocols of spectral domain optical coherence tomography to diagnose preperimetric glaucoma. Invest Ophthalmol Vis Sci. 2013;54(12):7252–7.

Seol BR, Jeoung JW, Park KH. Glaucoma detection ability of macular ganglion cell-inner plexiform layer thickness in myopic preperimetric glaucoma. Invest Ophthalmol Vis Sci. 2015;56(13):8306–13.

Shin JW, Sung KR, Lee GC, Durbin MK, Cheng D. Ganglion cell-inner plexiform layer change detected by optical coherence tomography indicates progression in advanced glaucoma. Ophthalmology. 2017;124(10):1466–74.

Shin JW, Sung KR, Park SW. Patterns of progressive ganglion cell-inner plexiform layer thinning in glaucoma detected by OCT. Ophthalmology. 2018;125(10):1515–25.

Shin JW, Sung KR, Song MK. Ganglion cell-inner plexiform layer and retinal nerve fiber layer changes in glaucoma suspects enable prediction of glaucoma development. Am J Ophthalmol. 2020;210:26–34.

Wollstein G, Schuman JS, Price LL, et al. Optical coherence tomography longitudinal evaluation of retinal nerve fiber layer thickness in glaucoma. Arch Ophthalmol. 2005;123(4):464–70.

Wu K, Lin C, Lam AK, Chan L, Leung CK. Wide-field trend-based progression analysis of combined retinal nerve fiber layer and ganglion cell inner plexiform layer thickness: a new paradigm to improve glaucoma progression detection. Ophthalmology. 2020;127(10):1322–30.

Yu M, Lin C, Weinreb RN, Lai G, Chiu V, Leung CK. Risk of visual field progression in glaucoma patients with progressive retinal nerve fiber layer thinning: a 5-year prospective study. Ophthalmology. 2016;123(6):1201–10.

Zhang X, Dastiridou A, Francis BA, et al. Comparison of glaucoma progression detection by optical coherence tomography and visual field. Am J Ophthalmol. 2017;184:63–74.